NASA TECHNICAL NOTE

NASA TN D-4967

NASA TN D-4967

AN ANALYTICAL METHOD FOR PREDICTING THE PERFORMANCE OF CENTRIFUGAL PUMPS DURING PRESSURIZED STARTUP

by Wojciech Rostafinski

Lewis Research Center

Cleveland, Ohio

NATIONAL AERONAUTICS AND SPACE ADMINISTRATION • WASHINGTON, D. C. • JANUARY 1969

AN ANALYTICAL METHOD FOR PREDICTING THE PERFORMANCE OF CENTRIFUGAL PUMPS DURING PRESSURIZED STARTUP

By Wojciech Rostafinski

Lewis Research Center
Cleveland, Ohio

NATIONAL AERONAUTICS AND SPACE ADMINISTRATION

For sale by the Clearinghouse for Federal Scientific and Technical Information
Springfield, Virginia 22151 – CFSTI price $3.00

ABSTRACT

The pressure drop characteristics of centrifugal pumps during pressurized startup were studied analytically. Mathematical expressions for negative head characteristics were developed and applied to the prediction of pressure drop characteristics for three pumps. Comparison of calculated and experimental performance points verified the analytical method developed.

AN ANALYTICAL METHOD FOR PREDICTING THE PERFORMANCE OF CENTRIFUGAL PUMPS DURING PRESSURIZED STARTUP

by Wojciech Rostafinski

Lewis Research Center

SUMMARY

The pressure drop characteristics of centrifugal pumps during pressurized startup were studied analytically. A method for predicting pump pressure drop characteristics was developed. Values were calculated for three pump configurations and compared with experimental data. Enough test data were available for the two pumps with vaned diffusers to verify the analytical method quantitatively. In the third case, a pump with a vaneless diffuser, the procedure was verified qualitatively.

The method developed is based on the analysis both of work done on the pump's impeller and of the hydraulic losses within a pump when it is subjected to flow forced by a pressurized tank. An empirical correction factor based on an analytical extrapolation of the data from the pump's high-speed characteristic is used to adjust the analytical equations for the generally unknown losses due to the mismatch of flow and blade angles at the entrance of the diffuser.

The close agreement of calculated and experimental performance points verifies the analytical method. The study demonstrates that it is possible to predict the pressure drop characteristic of centrifugal pumps with vaned diffusers provided that the high-speed characteristic is known. To predict the pressure drop characteristic of a centrifugal pump with a vaneless diffuser, knowledge of the high-speed characteristic is not required.

INTRODUCTION

In the development of the chemical and nuclear rocket engine systems, it is necessary to know system performance not only at the design point but also in a wide range of

the off-design conditions. The need for this information is particularly severe in the case of engine systems where the hydraulic losses in the pump during startup affect the engine transient characteristics.

In the case of the axial turbopumps, methods (ref. 1) are available to calculate pump characteristics in a range 80 to 120 percent of the design flow point. Also, an analytical method has been developed, verified by experiments, and published (ref. 2), for the prediction of pressurized startup performance of a multistage axial pump.

Prediction of the off-design operation of centrifugal pumps presents a more difficult problem, especially for pumps equipped with vaned diffusers. The difficulty lies in the lack of information on hydraulic losses at the discharge of centrifugal impellers and at the entrance to the diffusers.

The usual method of evaluating the performance of a centrifugal pump at and near the design point is based on a comparison of the design parameters with the parameters of a similar pump of known performance. For strong off-design conditions such as those near the shutoff or maximum capacity points, it is necessary to correlate the empirical data from tests on a diffuser similar to the diffuser used. For extreme off-design operating conditions encountered during pressurized startup, there are no diffuser loss test data and no performance prediction method is available.

In this report, analytical expressions are developed to describe pump performance during pressurized startup. These analytical methods are applied to the following pump designs: (1) a radial centrifugal pump with a vaned diffuser, (2) a centrifugal pump with an impeller blade exit angle of 60° and equipped with a vaned diffuser, and (3) a centrifugal pump with an impeller blade exit angle of 35° and equipped with a vaneless diffuser.

The pressure drop characteristics are calculated and compared with data from tests run on the first two pumps. An additional qualitative verification of the theory is obtained using the design data of the third pump.

APPROACH

The generalized characteristic of a pump extends from positive to negative pressure differences. A study of complete generalized characteristics is given in reference 3. Figure 1, derived from this study, shows the more important features of the generalized characteristics of turbopumps. The generalized variables are $\Delta P/N^2$ and $\dot{w}/N$. (All symbols are defined in appendix A.) There are three regions of pump operation during pressurized startup. Region A is called "the reversed turbine operation" region; the pump operates as a hydraulic turbine with the torque supplied by fluid fed from a pressurized tank. Impellers with a blade discharge angle other than 90° will act as a hydraulic turbine when subject to induced tank flow. The characteristic of such a hydraulic

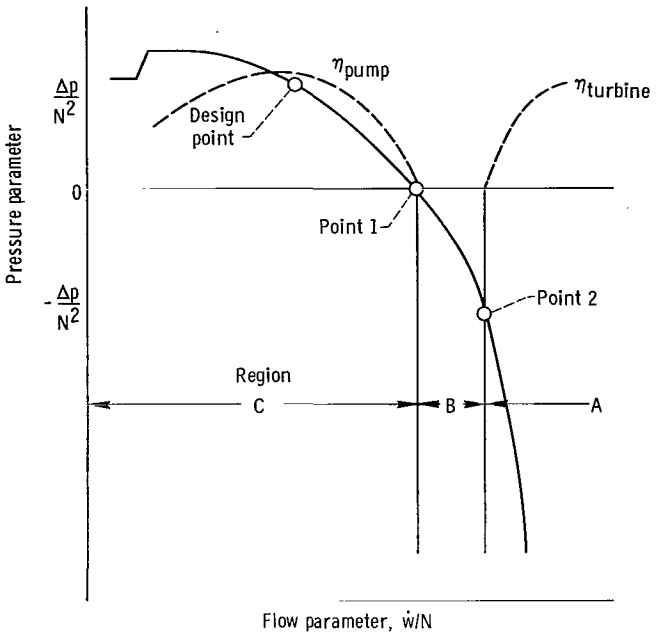

Figure 1. - Generalized pump characteristic extending into positive and negative pressure difference.

turbine can be calculated or can be obtained by tests. Region B is called "the energy dissipation region" where the torque is supplied by the flowing fluid and the primemover simultaneously. In this region, the pressure difference across the pump is still negative. Because the degree to which the primemover supplements the fluid torque is unknown, the characteristic in this region cannot be calculated. Region C is the pump operation region where a torque is applied to the pump by a primemover and there is a positive pressure difference across the pump. In this region, the pump characteristic may be approximately calculated or established by experiments.

There are two points in this figure which must be discussed. Point 1 is the pump zero-efficiency point. A pump reaches this point when the applied torque serves to balance the losses within the pump and no positive pressure difference is generated. Point 2 represents turbine (reverse hydraulic turbine) zero-efficiency point, that is, the zero-torque point or windmilling. At that point the impeller rotates at a speed that corresponds to the available pressure drop (inlet and outlet conditions) and is consistent with the flow that can be handled. At this point, no useful accelerating torque is available. The centrifugal pump characteristic (region C), to the right of the design point, has an increasingly negative slope. The hydraulic turbine characteristic (region A) is much steeper, and its slope varies little with the flow parameter $\dot{w}/N$. The two characteristics merge in region B where an adjustment of slopes must take place.

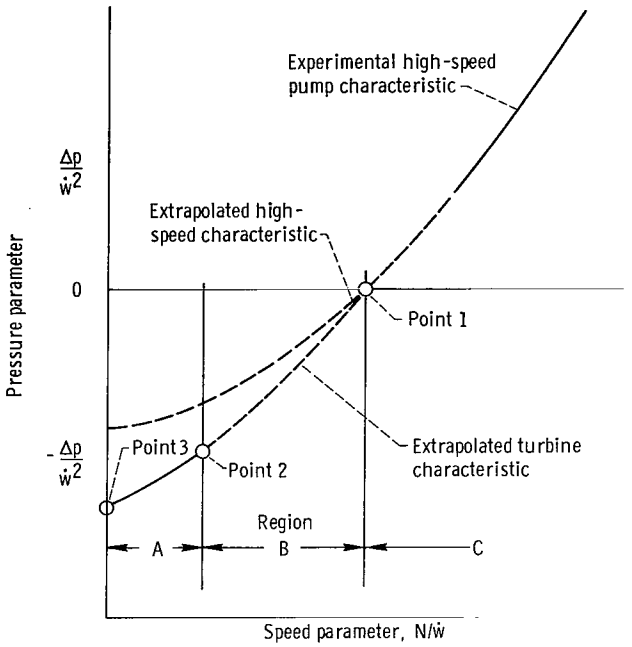

Figure 2. - Pump performance during pressurized startup for analytical model.

A more convenient form of the generalized characteristic for the startup calculation is shown in figure 2. The new variables are $\Delta P/\dot{w}^2$ and $N/\dot{w}$. The known pump characteristic and the calculated turbine characteristic are drawn as solid lines. The dashed lines represent analytical extrapolation of the pump characteristic beyond its experimental range and into regions B and A, and extrapolation of the turbine characteristic into region B. It is required that the turbine characteristic meet the pump characteristic at point 1. Because extrapolations are used, the two lines may not actually meet and, in practice, the requirement is that the two extrapolated characteristics must approach one another with the minimum deviation that can be found.

The path of the startup process between points 2 and 1 is not shown because it is essentially empirical; it should lie between the two dashed lines. Point 3 represents the locked rotor pressure drop or the pressure drop corresponding to the very initial moments of a startup process before any rotation is obtained. The location of point 2 depends on pump design. For an axial pump, point 2 is very close to point 3, as shown in appendix B where, from reference 2, the key results of a startup performance analysis for an axial pump are given. For a radial centrifugal pump, point 2 will be at point 3. For other designs, it will be anywhere between points 3 and 1. The ability to calculate the turbine characteristic or the zero-speed point for the radial pump makes it possible to define the complete pump startup characteristic.

DEVELOPMENT OF THE ANALYTICAL METHOD

Data Requirements

To calculate centrifugal pump startup characteristics, the following information must be available:

(1) The pump geometry including blade angles

(2) The design point flow, speed, and pressure rise

(3) The pump characteristic in a range within approximately ±10 percent of the design point flow.

To calculate the startup characteristic of an axial pump, the pump characteristic was not required; the velocity triangles at the design point were sufficient (ref. 2).

The difference between the analytical approach used in calculating the pressure loss characteristic of the axial pump of reference 2 and the approach needed for a centrifugal pump lies in the inability to predict losses resulting from the mismatch of the flow and diffuser blade angles of a centrifugal pump. However, with a known pump characteristic, the calculated startup characteristic may be adjusted for those losses by the use of a correction factor.

Head Characteristic

The energy equation for an incompressible and nonconducting fluid and for a steady adiabatic turbulent flow, where the change in potential energy due to change in height is neglected, is (ref. 4)

$$\Delta h_s = \frac{\Delta V^2}{2g} + \frac{g_c}{g} W + \frac{g_c}{g} \varphi \tag{1}$$

which states that the change of the static head equals the change of the kinetic energy (based on the average conduit velocity), the work done on or by the impeller W, and the viscous losses φ (the energy that is dissipated due to viscous effects per pound of fluid). Equation (1) expressed in terms of the total head change becomes

$$\Delta h = \frac{g_c}{g} W + \frac{g_c}{g} \varphi \tag{2}$$

The low-velocity hydraulic turbine flow criteria and a one-dimensional analysis, similar to the approach used in reference 5, are used to describe the flow dynamics of the system under consideration. Consequently, leakage, windage, and mechanical losses are neglected and the work done by the fluid on the impeller is considered negative.

To expand equation (1), use will be made of the fluid velocity components over blades. For simplicity, in subsequent equations, the parameter g_c will be replaced by g. Figure 3 gives station designations used in pump analysis.

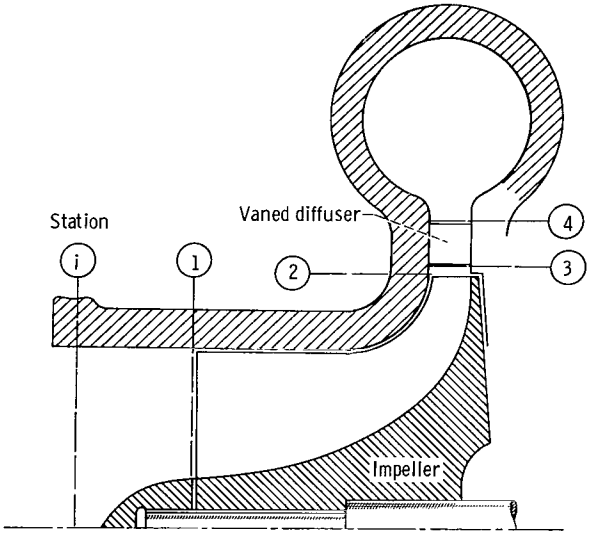

Figure 3. - Centrifugal pump station designation.

Change in Kinetic Energy

The change in kinetic energy is completely described by the pump inlet and the pump outlet velocity head difference $-\left(V_e^2 - V_i^2\right)/2g$ where V_e is the velocity at the pump discharge flange and V_i is the velocity in the inlet pipe.

Work

The work done by the fluid on the impeller must be described by the blade characteristics. The work done on the blades, by Euler's equation, is $-(u_1 V_{u,1} - u_2 V_{u,2})/g$.

Frictional Losses

The losses resulting from flow through the stage are of two types, losses due to friction and losses due to turbulence induced by the mismatch of blade and flow angles caused by the off-design operation. The frictional losses will be calculated using impeller and diffuser exit velocities. Actually, average fluid velocities in the flow passages should be used. Because the frictional losses during startup (low flows) are small compared with all other losses, the resulting error will be negligible. The frictional losses for the impeller and for the diffuser, respectively, are

$$-4f \frac{c}{d_h} \frac{V_2'^2}{2g} = -k_{f,r} \frac{V_2'^2}{2g}$$

$$-4f \frac{c}{d_h} \frac{V_4^2}{2g} = -k_{f,s} \frac{V_4^2}{2g}$$

where c is the mean-diameter blade length and d_h is the hydraulic diameter of the fluid passage formed by the average blade spacing s and the average blade height b. The friction coefficient f will be taken equal to 0.004, an average value over a wide range of Reynolds numbers (ref. 4), because as noted, the frictional losses are small.

Turbulence Losses

The turbulence losses which occur at the inlet of the impeller and the diffuser may be derived by analyzing the impeller inlet, impeller outlet, and diffuser inlet velocity triangles.

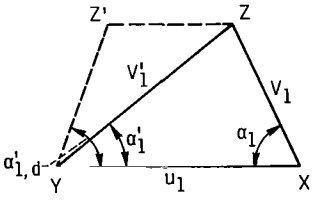

Figure 4. - Impeller inlet velocity triangle at off-design operation.

An efficient operation implies that the fluid angle α_1' will equal the design angle $\alpha_{1,d}'$. At off-design conditions, $\alpha_1' \neq \alpha_{1,d}'$. Consider an arbitrary impeller inlet velocity triangle XYZ as shown in figure 4. The fluid approaches the blades with a relative velocity V_1' at an angle α_1'. Because $\alpha_1' < \alpha_{1,d}'$, a tangential velocity component of adjustment ZZ' will be required to force the fluid to follow the blades. The energy loss resulting from this change of direction equals $-(ZZ')^2/2g$. From the geometry of the trapezoid XYZ'Z

$$ZZ' = u - \frac{\sin(\alpha_{1,d}' + \alpha_1)}{\sin \alpha_{1,d}'} V_1 = u_1 - k_r V_1$$

where

$$k_r = \frac{\sin(\alpha_{1,d}' + \alpha_1)}{\sin \alpha_{1,d}'}$$

and the loss is

$$-\frac{(u_1 - k_r V_1)^2}{2g}$$

Similarly the diffuser entrance loss may be evaluated in terms of the impeller outlet relative velocity V_2' and of the tip blade speed u_2, corrected for the diffusion effects in the annular space between impeller tip and the diffuser base circle. The velocity triangle at station 2 will be recalculated for station 3 by multiplying the tangential velocity components and the axial velocity by ratio r_2/r_3.

The diffuser entrance loss will be

$$-\frac{(u_3 - k_s V_3')^2}{2g}$$

which is $-(u_2 - k_s V_2')^2/2g$ adjusted for free vortex diffusion between stations 2 and 3. The loss coefficient is

$$k_s = \frac{\sin(\alpha_3' + \alpha_{3,d})}{\sin \alpha_{3,d}}$$

By a simple trigonometric transformation it may be shown that $k_r = u_1/V_1$ and $k_s = u_3/V_3'$ which indicates that turbulence loss calculation assumes no loss at the pump design point operation and assumes a definite incidence angle at which this occurs. While this is of no consequence with the impeller inlet loss, it is generally not the case with the diffuser inlet loss.

Experimental data reported in appendix C indicate that diffuser inlet losses may be important. In this experimental work, generally the diffuser loss is never zero and the minimum loss, depending on design, may be significant. Furthermore, the incidence at which this minimum occurs depends on pump and diffuser blade configuration. Examination of the design parameters of the diffusers under consideration indicate that the incidence related to the minimum loss and the corresponding pressure drop cannot be correlated with the design data. A successful correlation would require an extensive study of different designs. For the same reason, the losses at off-design conditions are even more difficult to evaluate. A further complication arises from the fact that pump design point (best efficiency) seldom coincides with the minimum diffuser inlet loss.

This lack of information on the diffuser entrance loss requires that an empirical correction factor λ must be used to adjust k_s to a new loss coefficient $K_s = \lambda k_s$.

Stage Exit Loss

It will be assumed that except for $V_e^2/2g$ all velocity head at discharge from the diffuser (vaned or vaneless) is lost. The loss will be equal to $(V_4^2 - V_e^2)/2g$.

Generalized Negative Head Characteristic

By use of the relations obtained for the work done and for the various losses, equation (1) becomes

$$2g\,\Delta h_s = V_i^2 - V_e^2 - (V_4^2 - V_e^2) - \left[(k_{f,s}V_4^2 + k_{f,r}V_2'^2) + 2(u_1V_{u,1} - u_2V_{u,2}) + (u_1 - k_rV_1)^2 + (u_3 - k_sV_3')^2\right] \qquad (3)$$

To express the head loss in terms of V_1 and u_1 only, the following relations, derived from the velocity triangles will be used:

$$V_{u,1} = \begin{cases} V_1 \cos \alpha_1 \\ 0 \text{ for } \alpha_1 = 90^o \end{cases}$$

$$V_{u,2} = u_2 - V_2' \cos \alpha_2'$$

$$V_2^2 = u_2^2 + V_2'^2 - 2u_2 V_2' \cos \alpha_2'$$

$$V_{u,2} r_2 = V_{u,3} r_3$$

In addition, it will be convenient to eliminate V_2' by writing $V_2' = yV_1$ where y is a proportionality constant. The two velocities V_2' and V_1 are always proportional to each other because for any given slip their orientation is fixed. Now since $N = 30u/\pi r$ (in SI units, $N = u/r$) and by continuity equation $Q = \Omega_1 V_1 \sin \alpha_1$, the expression for negative head characteristic may be written in measurable quantities such as N and Q instead of the corresponding velocities u_1 and V_1.

After substituting and rearranging, the head parameter $\Delta h_s/Q^2$ of the pump is expressed as a function of the speed parameter N/Q and a number of design parameters as follows:

$$\frac{\Delta h_s}{Q^2} = \frac{1}{2g\Omega_i^2} - \frac{1}{2g\Omega_e^2} - \left(\frac{1}{8g\pi^2 r_4^2 b_4^2 \sin^2 \alpha_4} - \frac{1}{2g\Omega_e^2} \right) - \left\{ \frac{k_{f,s}}{8\pi^2 g r_4^2 b_4^2 \sin^2 \alpha_4} + \frac{y^2 k_{f,r}}{2g\Omega_1^2 \sin^2 \alpha_1} + \frac{k_r^2}{2g\Omega_1^2 \sin^2 \alpha_1} \right.$$

$$+ \left(\frac{r_2}{r_3} \right)^2 \frac{k_s^2}{2g} \left(\frac{y^2 \cos^2 \alpha_2'}{\Omega_1^2 \sin^2 \alpha_1} + \frac{1}{4\pi^2 r_2^2 b_3^2} \right) + \frac{\pi r_1}{30g\Omega_1 \sin \alpha_1} \left[\cos \alpha_1 + y \left(\frac{r_2}{r_1} \right) \cos \alpha_2' - k_r - \sin \alpha_1 \Omega_1 \left(\frac{r_2}{r_1} \right) \left(\frac{r_2}{r_3} \right)^2 \right.$$

$$\left. \left. \times k_s \sqrt{\frac{y^2 \cos^2 \alpha_2'}{\Omega_1^2 \sin^2 \alpha_1} + \frac{1}{4\pi r_2^2 b_3^2}} \right] \left(\frac{N}{Q} \right) + \frac{\pi^2 r_1^2}{1800g} \left[1 + \left(\frac{r_2}{r_1} \right) \left(\frac{r_2}{r_3} \right)^2 - 2 \left(\frac{r_2}{r_1} \right)^2 \right] \left(\frac{N}{Q} \right)^2 \right\} \qquad (4a)$$

In special cases, this equation simplifies greatly. If the diffuser is located in the immediate vicinity of the rotor tip $r_2 = r_3$ and no diffusion need be considered; for a pump equipped with a vaneless diffuser $k_s = 0$ and also $r_3 = r_2$. In the SI system of units, this equation becomes

$$\frac{\Delta h_s}{Q^2} = \frac{1}{2g\Omega_i^2} - \frac{1}{2g\Omega_e^2} - \left(\frac{1}{8g\pi^2 r_4^2 b_4^2 \sin^2 \alpha_4} - \frac{1}{2g\Omega_e^2}\right) - \left\{\frac{k_{f,s}}{8g\pi^2 r_4^2 b_4^2 \sin^2 \alpha_4} + \frac{y^2 k_{f,r}}{2g\Omega_1^2 \sin^2 \alpha_1} + \frac{k_r^2}{2g\Omega_1^2 \sin^2 \alpha_1}\right.$$

$$+ \left(\frac{r_2}{r_3}\right)^2 \frac{k_s^2}{2g}\left(\frac{y^2 \cos^2 \alpha_2'}{\Omega_1^2 \sin^2 \alpha_1} + \frac{1}{4\pi^2 r_2^2 b_3^2}\right) + \frac{r_1}{g\Omega_1 \sin \alpha_1}\left[\cos \alpha_1 + y\left(\frac{r_2}{r_1}\right)\cos \alpha_2' - k_r - \sin \alpha_1 \Omega_1 \left(\frac{r_2}{r_1}\right)\left(\frac{r_2}{r_3}\right)^2\right.$$

$$\left.\left. \times k_s \sqrt{\frac{y^2 \cos^2 \alpha_2'}{\Omega_1^2 \sin^2 \alpha_1} + \frac{1}{4\pi^2 r_2^2 b_3^2}}\right]\left(\frac{N}{Q}\right) + \frac{r_1^2}{2g}\left[1 + \left(\frac{r_2}{r_1}\right)^2\left(\frac{r_2}{r_3}\right)^2 - 2\left(\frac{r_2}{r_3}\right)^2\right]\left(\frac{N}{Q}\right)^2\right\} \qquad (4b)$$

Equations (4) are applicable to single-stage centrifugal pumps. If a multistage centrifugal pump is considered, all terms in these equations, except the first two, will be written for each stage using appropriate velocity triangles.

Equation (4a) is the final general expression for the negative head characteristic of centrifugal pumps in terms of head difference Δh_s and volumetric flow Q. For practical applications, it will be more convenient to use pressure drop and speed parameters, $\Delta P/\dot{w}^2$ and $N/\dot{w}$, respectively.

Equation (4a) will be applied directly by assuming that there is no slip. This assumption may be justified as follows: in radial centrifugal pumps the fluid will discharge from the impeller at the blade angle of 90° with no tangential component capable of producing a starting torque. For a blade discharge angle other than 90° the initial torque will tend to rotate the pump but will be opposed by friction. The mechanical losses such as bearing friction, not considered in the analysis, may however, prevent the rotation. Once the rotation is set in, the slip, if any, will be small and may be disregarded.

The blockage due to the number of blades must be accounted for. It will influence the shape and size of the velocity triangle at the impeller discharge and must be carefully calculated.

Point of Zero Work Done on Impeller

By equating to zero the work term of the negative head characteristic and by making proper substitutions and rearrangements, the value of the speed parameter N/Q for the

zero-work point or the zero-torque point as it will be called, may be calculated from

$$(u_1 V_{u,1} - u_2 V_{u,2}) = \frac{Q}{\Omega_1 \sin \alpha_1}(r_1 \cos \alpha_1 + r_2 y \cos \alpha_2') - \frac{\pi r_2^2}{30} N = 0 \qquad (5a)$$

which, for axial inlet to the rotor ($\alpha_1 = 90^\circ$), simplifies to

$$\frac{N}{Q} = \frac{30g \cos \alpha_2'}{\pi \Omega_1 r_2} \qquad (5b)$$

In the SI system of units these two equations are unchanged except that the factor $30/\pi$ drops out because it is contained in N. For radial blading when slip is not considered, $\alpha_2' = 90^\circ$ and $N/Q = 0$; that is, there will be no windmilling and a torque from the turbine is necessary to start the rotation.

VERIFICATION OF THE ANALYTICAL METHOD

Mark III - Model IV Turbopump

Data. - Based on experimental data, the high-speed pump map (unpublished data from Aerojet-General Corp.) is shown in figure 5(a). The generalized characteristic can be described by the curve-fit equation

$$\frac{\Delta p}{\dot{w}^2} = -0.0435 + \frac{0.319}{10^3}\left(\frac{N}{\dot{w}}\right) + \frac{1.379}{10^6}\left(\frac{N}{\dot{w}}\right)^2$$

which becomes the following in SI units (Note: In all cases that follow, the second of the two equations for $\Delta h/Q^2$ or for $\Delta p/\dot{w}^2$ is the equation in SI units.):

$$\frac{\Delta p}{\dot{w}^2} = -0.146 + \frac{4.62}{10^3}\left(\frac{N}{\dot{w}}\right) + \frac{86.75}{10^6}\left(\frac{N}{\dot{w}}\right)^2$$

This curve is shown as the solid line in figure 5(b). The dashed line represents a plot of points calculated from the equation for the region below the experimental range, from $N/w = 185$ (42.5) down to $N/\dot{w} = 0$.

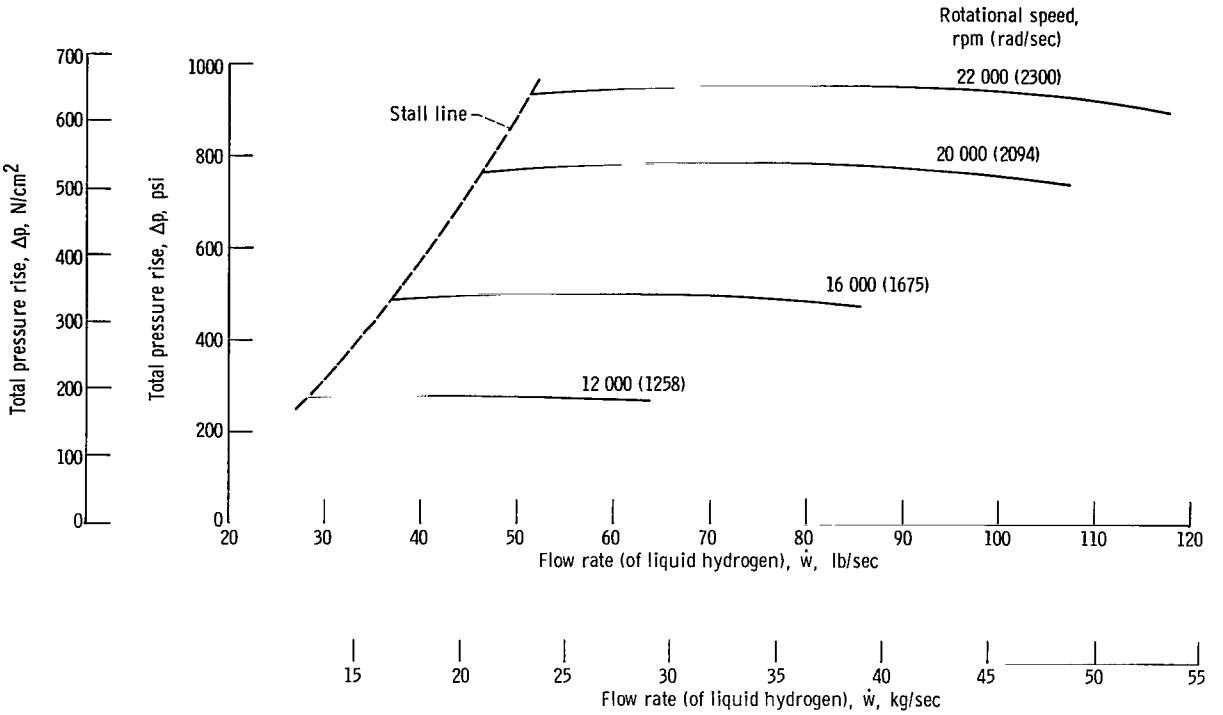

(a) Experimental high-speed performance map.

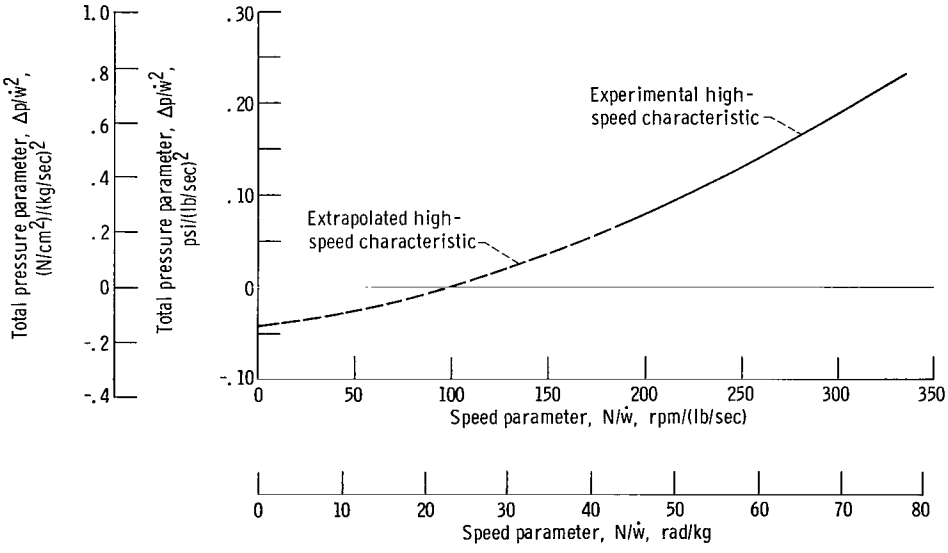

(b) Generalized performance characteristic.

Figure 5. - Experimental high-speed performance map and generalized performance characteristic for Mark III - Model IV turbopump.

The pump rotor consists of an inducer followed by radial blades. Pump design data and the geometry of the pump are as follows:

Inlet tip diameter, in. (cm)	6.95 (17.65)
Inlet hub diameter, in. (cm)	1.65 (4.19)
Rotor tip diameter, in. (cm)	12.25 (31.11)
Diffuser inlet diameter, in. (cm)	12.68 (32.21)
Diffuser discharge diameter, in. (cm)	16.28 (41.35)
Inducer inlet blade angle, deg	7
Rotor tip blade angle, deg	90
Diffuser blade angle, deg	9.25
Rotor tip port, in. (cm)	0.485 (1.23)
Diffuser port, in. (cm)	0.550 (1.40)
Rotor number of blades (discharge)	48
Diffuser number of blades	8
Rotor blade blockage (discharge), percent	29.5
Discharge pipe diameter, in. (cm)	4.83 (12.27)
Nominal speed, rpm (rad/sec)	22 500 (2356)
Nominal flow (liquid hydrogen), lb/sec (kg/sec)	75 (34.2)

Pressure drop characteristic. - The mean blade inlet and exit velocity triangles for the design point operation and for zero slip are shown in figure 6. The evaluation of constants yields

$$y = V_2'/V_1 = 2.26$$

$$k_r = u_1/V_1 = 5.75$$

$$k_s = u_2/V_2' = 7.1$$

Evaluation of friction losses gives $k_{f,r} = 0.466$ and $k_{f,s} = 0.070$. Using equation (4a) with $r_3 = r_2$ for a diffuser located directly at the discharge of the impeller blades, the generalized negative head characteristic is

$$\frac{\Delta h}{Q^2} = -70.1 + 0.119\left(\frac{N}{Q}\right) + \frac{0.214}{10^4}\left(\frac{N}{Q}\right)^2$$

$$\frac{\Delta h}{Q^2} = -2.67\times10^4 + 12.23\left(\frac{N}{Q}\right) + \frac{5.94}{10^4}\left(\frac{N}{Q}\right)^2$$

The term of equation (4a) containing $k_{f,s}$ is $-1.1(-0.042\times10^4)$ and the term containing $k_{f,r}$ is $-0.6(-0.023\times10^4)$. During startup, the fluid friction effects are very small. To simplify analysis, these two terms will be neglected in all future calculations.

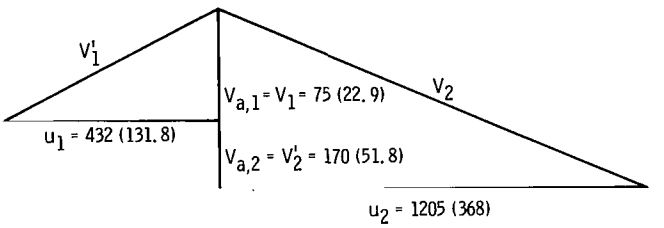

Figure 6. - Velocity triangles for design point operation and no slip assumption for Mark III - Model IV turbopump. (All velocities are given in ft/sec (m/sec).)

The generalized negative head characteristic recalculated for liquid hydrogen (specific gravity = 0.07) and written as the pressure drop characteristic in terms of $\Delta p/\dot{w}^2$ and $N/\dot{w}$ is

$$10^2\frac{\Delta p}{\dot{w}^2} = -11.15 + 0.0826\left(\frac{N}{\dot{w}}\right) + \frac{0.655}{10^4}\left(\frac{N}{\dot{w}}\right)^2$$

$$10^2\frac{\Delta p}{\dot{w}^2} = -37.35 + 1.198\left(\frac{N}{\dot{w}}\right) + \frac{41.18}{10^4}\left(\frac{N}{\dot{w}}\right)^2$$

The pump characteristic and the calculated pressure drop characteristic (marked $\lambda = 1$) are shown in figure 7. The two characteristics do not approach closely at the line $\Delta p = 0$ as they should. With the assumption of no mechanical losses, this indicates that the diffuser entrance losses at the design point are not negligible or that the incidence of the minimum is different from that assumed by taking $\lambda = 1$. By trial and error, when the correction factor λ is assigned a value such that $K_s = \lambda k_s = 0.45\ k_s$, the result is a curve (shown in fig. 7 and marked $\lambda = 0.45$) which nearly meets the extrapolated characteristic at $\Delta p = 0$.

The new pressure drop characteristic is

$$10^2 \frac{\Delta p}{\dot{w}^2} = -5.40 + 0.048 \left(\frac{N}{\dot{w}}\right) + \frac{0.655}{10^4} \left(\frac{N}{\dot{w}}\right)^2$$

$$10^2 \frac{\Delta p}{\dot{w}^2} = -18.1 + 0.697 \left(\frac{N}{\dot{w}}\right) + \frac{41.18}{10^4} \left(\frac{N}{\dot{w}}\right)^2$$

By equation (5a), the zero-torque or windmilling point is at $N/\dot{w} = 0$, that is, at this point fluid fed by a pressurized tank will not initiate rotation. Furthermore, the calculated characteristic lies entirely (except for the point $N/\dot{w} = 0$) in the power dissipation zone, and the actual pump operation points will be located above the calculated curve.

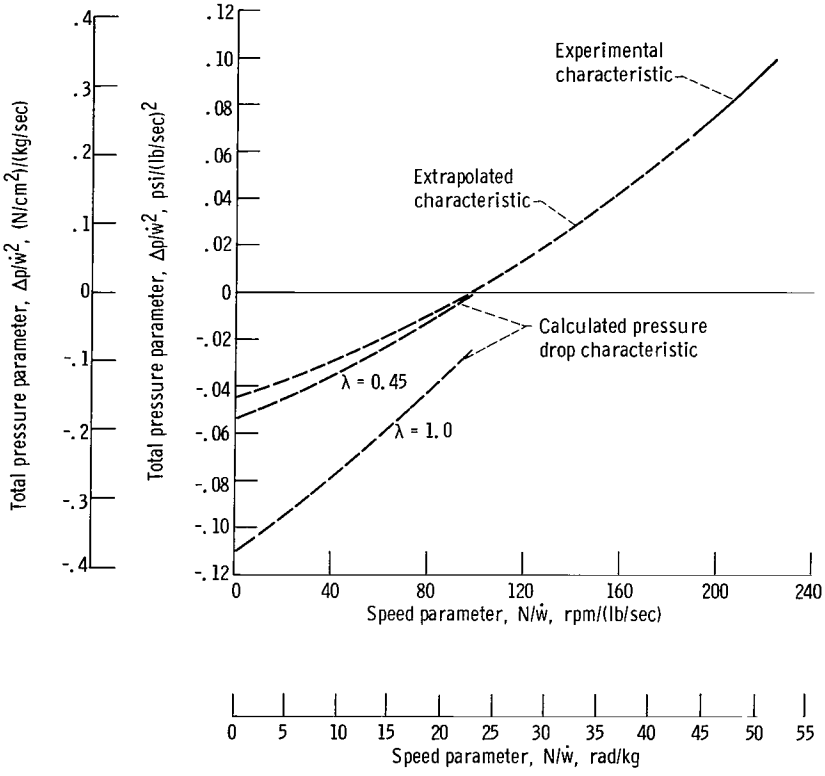

Figure 7. - Determination of startup characteristic for Mark III - Model IV turbopump.

Comparison of experimental and calculated data. - Two types of tests were conducted on the Mark III - Model IV turbopump. In the first, liquid hydrogen was forced through the pump using only tank pressure. No power was applied through the turbine. In the second type of tests, high pressure hydrogen gas powered the turbine and the turbine discharge to a subatmospheric vent at 12 pounds per square inch absolute (8.3 N/cm^2 abs). A speed control loop manipulated the turbine power control valve to hold speed constant.

For both types of tests, a remotely controlled pump discharge valve was used to load the pump.

The results of the first type of tests are shown in figure 8; no rotation was initiated in spite of strong pressurization of the run tank. The curve fit of the experimental data for pressure drop across the pump during the zero rotation test is $\Delta p_s/\dot{w}^2 = -0.057$ (-0.191) and $\Delta p/\dot{w}^2 = -0.545$ (-0.183).

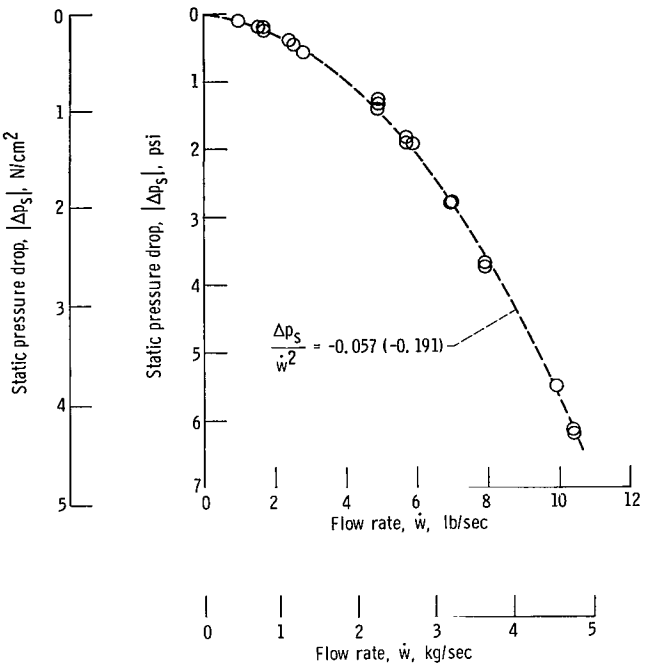

Figure 8. - Pressure drop at zero speed for Mark III - Model IV turbopump.

The results of the second test are shown in figure 9. The setup with the turbine connected to the exhaust system allowed the leakage from the pump bearing to expand in the turbine rows. Some torque was supplied to the impeller to drive the pump, and rotation was initiated. The experimental data show a gradual decrease in pressure drop across the pump as speed increased. During several runs, tank pressure was varied from 35 to 50 pounds per square inch (24.1 to 34.5 N/cm^2) with no apparent influence on startup performance. It should be noted that the experimental points in the negative Δp-zone cannot be connected by a simple segment of a parabola.

In the same figure, the calculated curves from figure 7 are shown, and the relation between the predicted operation points and the experimental data is displayed. The zero-speed point pressure drop parameter is $\Delta p/\dot{w}^2 = -0.0545$ (-0.183) while the calculated $\Delta p/\dot{w}^2 = -0.054$ (-0.181).

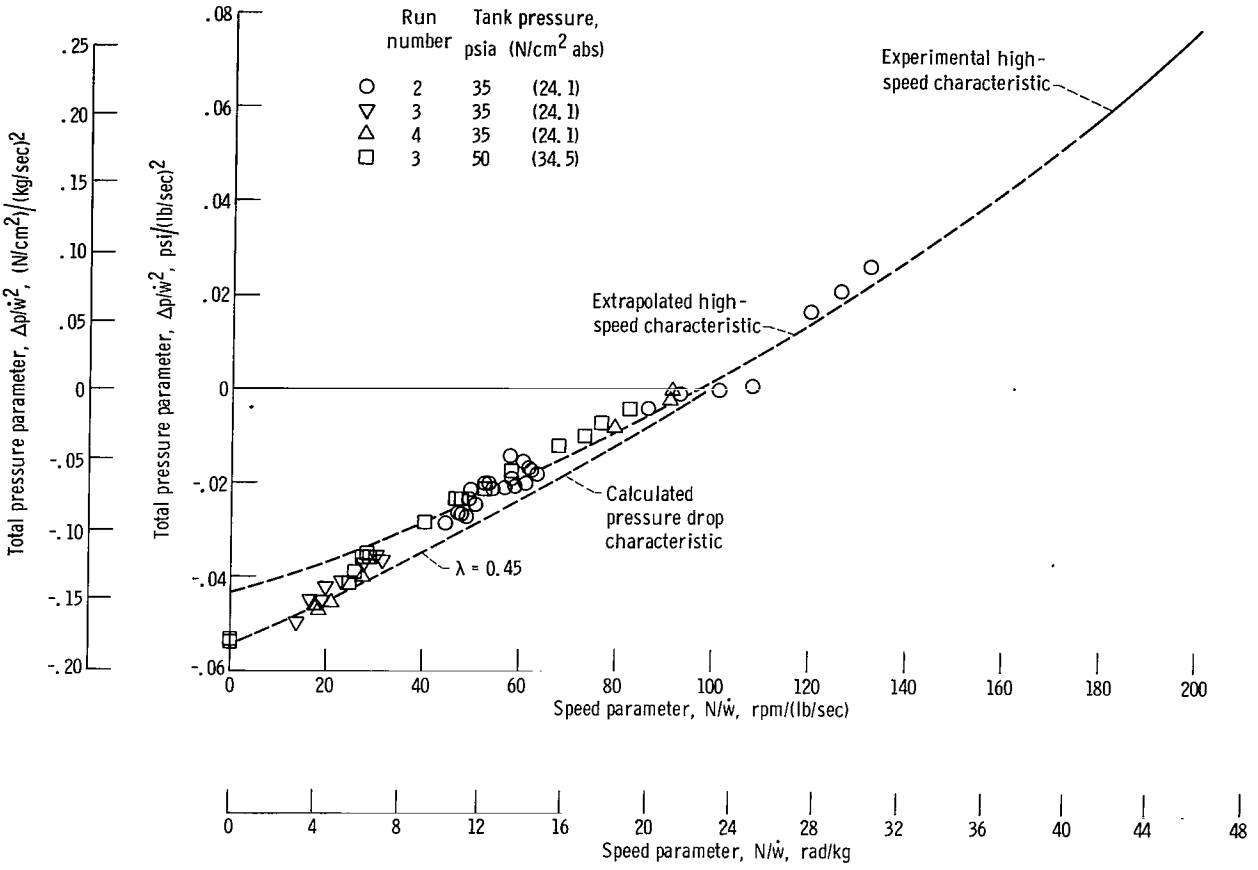

Figure 9. - Verification of analytically established characteristic for pressurized startup of Mark III - Model IV turbopump.

Figure 9 is similar to figure 15 (refer to appendix B) where the pressurized startup test data and calculated characteristic of an axial pump are shown. In both figures, there is a discontinuity of the slope of the pump and pressurized startup characteristics; in both cases, the pressure drop and the extrapolated pump characteristics approximately meet at the line $\Delta p = 0$. Also, the actual zero-speed points are located below the zero-speed points obtained by extrapolation of the high-speed characteristic.

Mark 29F Turbopump

Data. - The predicted and the experimental high-speed map of the Mark 29F liquid hydrogen turbopump (unpublished data from the Rocketdyne Division of North American Rockwell Corp.) is shown in figure 10(a). The generalized characteristic calculated by means of the experimental data, in terms of $N/\dot{w}$ and $\Delta p/\dot{w}^2$, is

$$\frac{\Delta p}{\dot{w}^2} = -0.0875 + \frac{0.350}{10^3}\left(\frac{N}{\dot{w}}\right) + \frac{1.87}{10^6}\left(\frac{N}{\dot{w}}\right)^2$$

$$\frac{\Delta p}{\dot{w}^2} = -0.293\times10^2 + \frac{5.08}{10^3}\left(\frac{N}{\dot{w}}\right) + \frac{117.6}{10^6}\left(\frac{N}{\dot{w}}\right)^2$$

This curve is shown as the solid line in figure 10(b). The dashed line represents the analytically extrapolated high-speed characteristic below the experimental range down to $N/\dot{w} = 0$.

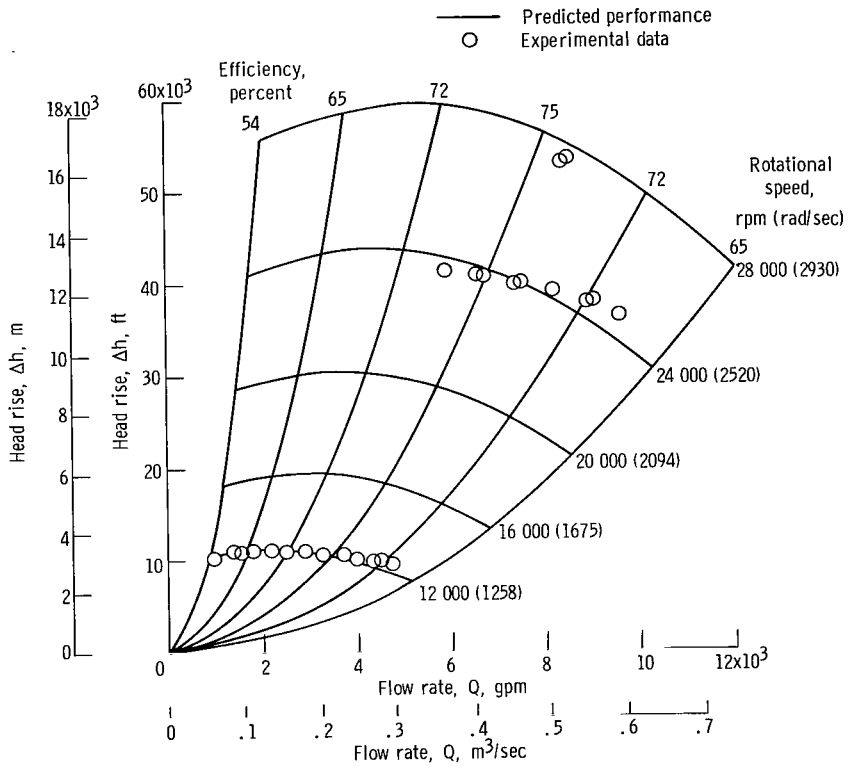

(a) Experimental performance map.

Figure 10. - Experimental performance map and generalized high-speed and calculated pressure drop characteristics for Mark 29F turbopump.

Pump design data and more important geometry data (unpublished data from the Rocketdyne Division of North American Rockwell Corp.) are as follows:

Inducer inlet tip diameter, in. (cm)	8.15 (20.70)
Inducer inlet hub diameter, in. (cm)	3.20 (8.13)
Inducer discharge tip diameter, in. (cm)	9.00 (22.86)
Inducer discharge hub diameter, in. (cm)	7.50 (19.05)
Impeller inlet tip diameter, in. (cm)	6.80 (17.27)
Impeller inlet hub diameter, in. (cm)	4.50 (11.43)
Impeller tip diameter, in. (cm)	11.50 (29.21)
Diffuser base circle diameter, in. (cm)	12.20 (31.00)
Diffuser discharge diameter, in. (cm)	14.50 (36.80)
Inducer mean flow angle at exit, deg	30
Diffuser mean blade angle at discharge, deg	59.3
Impeller tip blade angle, deg	60
Diffuser blade angle at discharge, deg	12.8
Nominal speed, rpm (rad/sec)	28 000 (2932)
Nominal flow, gpm (m^3/sec)	10 116 (0.638)

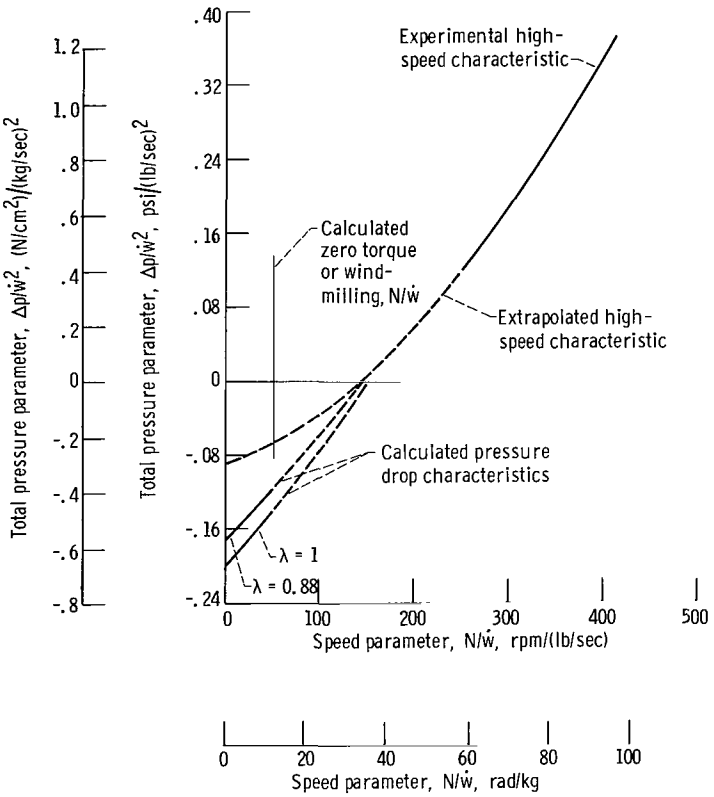

(b) Experimental generalized high-speed and calculated pressure drop characteristics.

Figure 10. - Concluded.

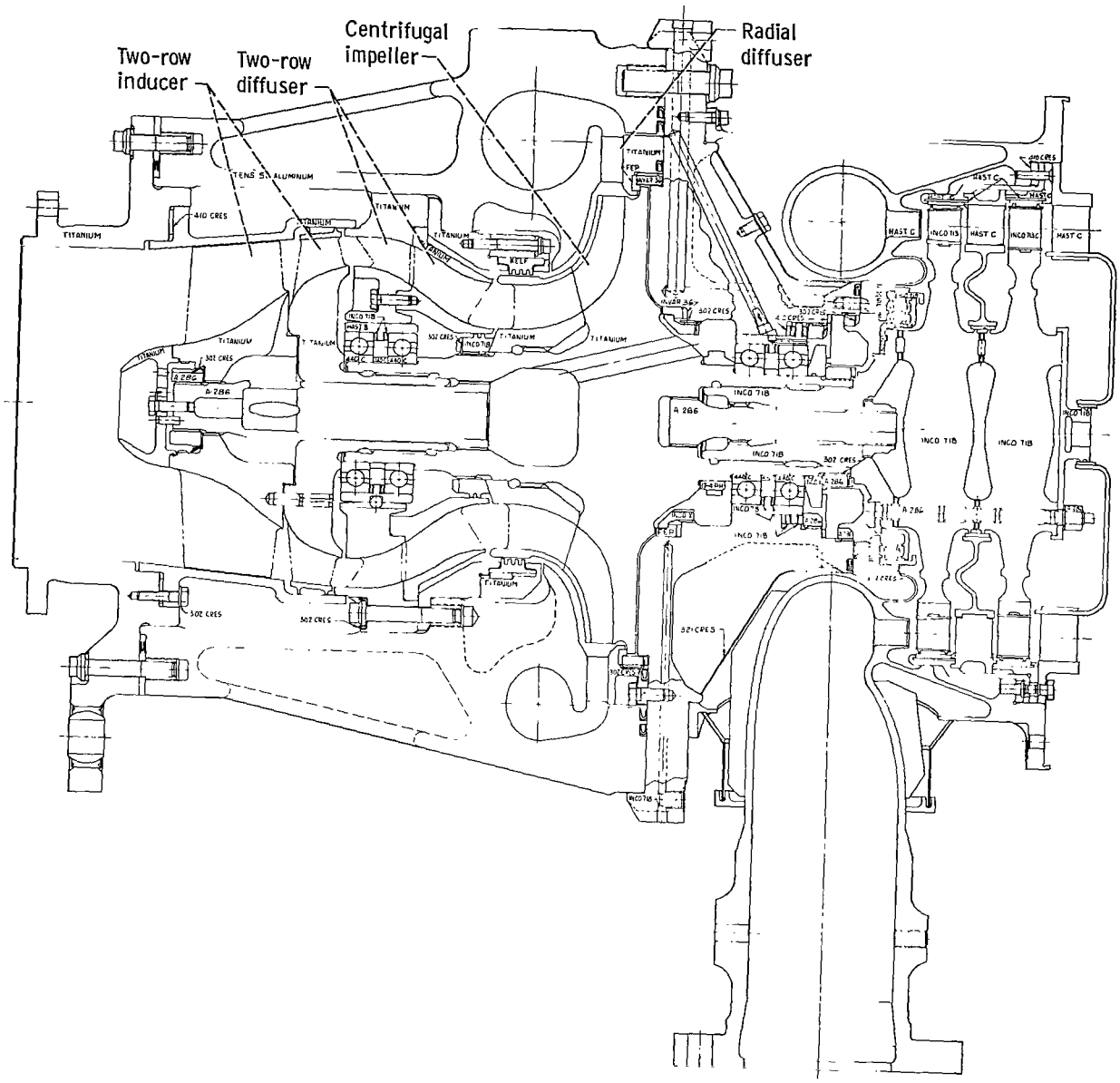

Figure 11. - Cross section of Mark 29F turbopump. CD-10096-28

Because the configuration of this pump is very special, its cross section is shown in figure 11. The pump consists of an inducer followed by a long diffuser which feeds a centrifugal impeller. The impeller discharges into a radial diffuser. The inducing stage has a two-row rotor and stator. This special feature is of no consequence in the present analysis which considers only the inlet and outlet velocity triangles.

Pressure drop characteristic. - The velocity triangles for the inducer and the centrifugal stages are established using unpublished data from the Rocketdyne Division of North American Rockwell Corporation. The negative head characteristic for the inducer stage is calculated using the equation reported in reference 1. The design point deviation is assumed, and friction losses are neglected. The result is

$$\frac{\Delta h}{Q^2} = -45.3 + 0.0557\left(\frac{N}{Q}\right) + \frac{0.0105}{10^3}\left(\frac{N}{Q}\right)^2$$

$$\frac{\Delta h}{Q^2} = -1.78\times10^4 + 5.72\left(\frac{N}{Q}\right) + \frac{0.292}{10^3}\left(\frac{N}{Q}\right)^2$$

The centrifugal stage negative head characteristic is calculated using equation (4a) and the assumption of zero slip. The calculated head drop includes the discharge losses. The result is

$$\frac{\Delta h}{Q^2} = -82.80 + 0.1035\left(\frac{N}{Q}\right) + \frac{0.0338}{10^3}\left(\frac{N}{Q}\right)^2$$

$$\frac{\Delta h}{Q^2} = -3.15\times10^4 + 10.65\left(\frac{N}{Q}\right) + \frac{0.94}{10^3}\left(\frac{N}{Q}\right)^2$$

The flow in the long diffuser between the inducer and the centrifugal impeller need not be considered because only total head changes are calculated and the friction losses are neglected.

Adding the partial results and converting Δh and Q into Δp and $\dot{w}$ using a specific gravity of 0.07 for liquid hydrogen yield the following for the Mark 29F pump:

$$\frac{\Delta p}{\dot{w}^2} = -0.200 + \frac{1.105}{10^3}\left(\frac{N}{\dot{w}}\right) + \frac{1.34}{10^6}\left(\frac{N}{\dot{w}}\right)^2$$

$$\frac{\Delta p}{\dot{w}^2} = -0.67\times10^2 + \frac{16.0}{10^3}\left(\frac{N}{\dot{w}}\right) + \frac{84.4}{10^6}\left(\frac{N}{\dot{w}}\right)^2$$

This curve does not meet the extrapolated high-speed characteristic at $\Delta p = 0$. Applying the correction factor $\lambda = 0.88$ gives the new pressure drop characteristic as

$$\frac{\Delta p}{\dot{w}^2} = -0.170 + \frac{0.99}{10^3}\left(\frac{N}{\dot{w}}\right) + \frac{1.34}{10^6}\left(\frac{N}{\dot{w}}\right)^2$$

$$\frac{\Delta p}{\dot{w}^2} = -0.57 + \frac{14.3}{10^3}\left(\frac{N}{\dot{w}}\right) + \frac{84.4}{10^6}\left(\frac{N}{\dot{w}}\right)^2$$

This curve does meet the extrapolated high-speed characteristic as required. By equation (5a), the zero-torque or windmilling point of the rotor assembly is located at $N/\dot{w} = 52.4$ (12.1). Evaluated separately for the inducer, it is $N/\dot{w} = 99$ (22.9); and for the centrifugal impeller alone, it is $N/\dot{w} = 30.3$ (7.0). These results are in agreement with the type of rotor considered. A nearly axial blading will exhibit a high $N/\dot{w}$ number, while a nearly radial centrifugal impeller will have a much smaller zero-torque point.

Comparison of experimental and calculated data. - Startup experiments on the Mark 29F pump were done (unpublished data from the Rocketdyne Division of North American Rockwell Corp.), and the performance data are reproduced in figure 12. The two curves give the pressure drop for a range of flows at windmilling and at zero speed (locked rotor). Because the tests were run with liquid hydrogen at several temperatures, the density of the hydrogen varied, and the pressure drop parameter $\Delta p/\dot{w}^2$ is not a constant. For the locked rotor tests, it varies between -0.164 and -0.171 (-0.55 and -0.574); and for windmilling test, it varies between -0.107 and -0.111 (-0.359 and -0.372).

Figure 13 gives a comparison of the calculated and the experimental data. The calculated curve with the correction factor $\lambda = 0.88$ meets the extrapolated high-speed characteristic on the $\Delta p = 0$ line as required. The experimental locked rotor pressure drop data verify the calculated point. The windmilling experimental data are located only slightly below the corresponding point given by the calculated characteristic and show generally good agreement with the calculated curve over the limited range available.

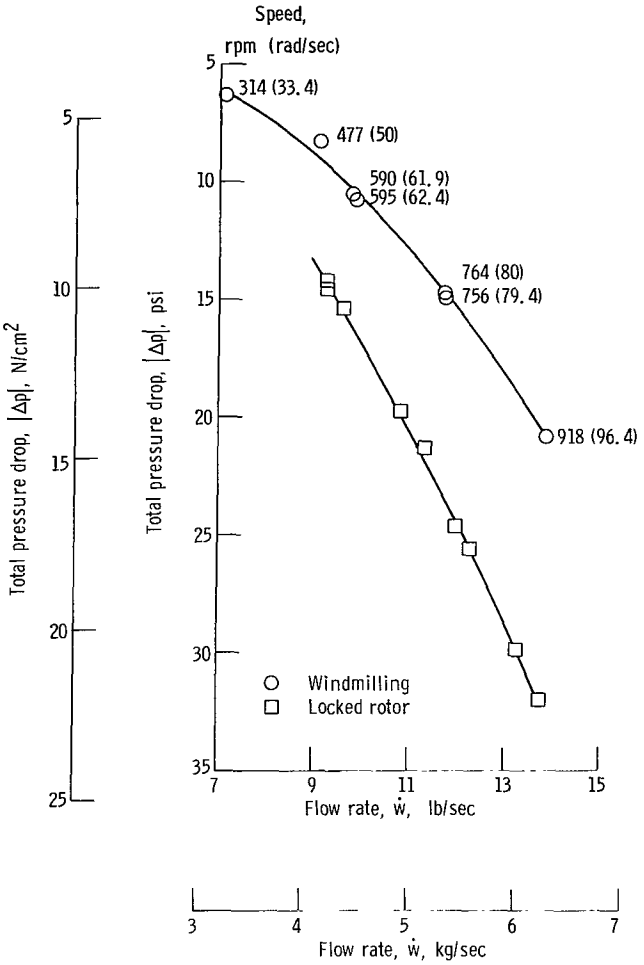

Figure 12. - Pressure drop at zero speed (locked rotor) and at windmilling for Mark 29F turbopump. Test fluid, liquid hydrogen.

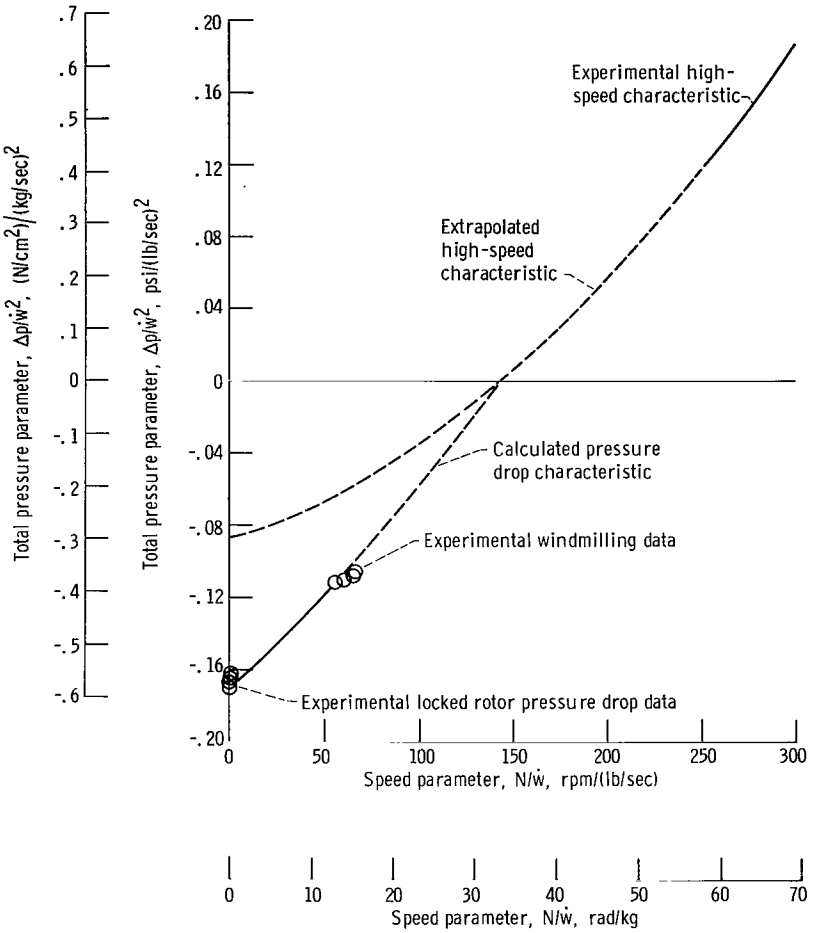

Figure 13. - Verification of analytically established characteristic for pressurized startup of Mark 29 F turbopump. Test fluid, liquid hydrogen.

M-1 Oxidizer Turbopump

To illustrate more completely the use of the developed equations and to verify the analytical approach, the pressure drop characteristic was calculated for a vaneless diffuser pump. The pump is a 3/8 scale model of the M-1 liquid oxygen centrifugal pump. This scale pump had been tested at high speed in water, but there was no information available on its startup performance. Consequently, the conclusions of this study can be qualitative only.

Data. - The M-1 scale pump has an axial flow inducer followed by radial vanes and its impeller is equipped with back vanes for axial thrust control. The experimental head characteristic of this pump in cold water from unpublished data of Aerojet-General Corporation is shown in figure 14(a). This characteristic corresponds to the following pressure drop characteristic:

$$10^3 \frac{\Delta p}{\dot{w}^2} = -2.478 - \frac{11.63}{10^3}\left(\frac{N}{\dot{w}}\right) + 0.01565\left(\frac{N}{\dot{w}}\right)^2$$

$$10^3 \frac{\Delta p}{\dot{w}^2} = -8.3 - 0.169\left(\frac{N}{\dot{w}}\right) + 0.98\left(\frac{N}{\dot{w}}\right)^2$$

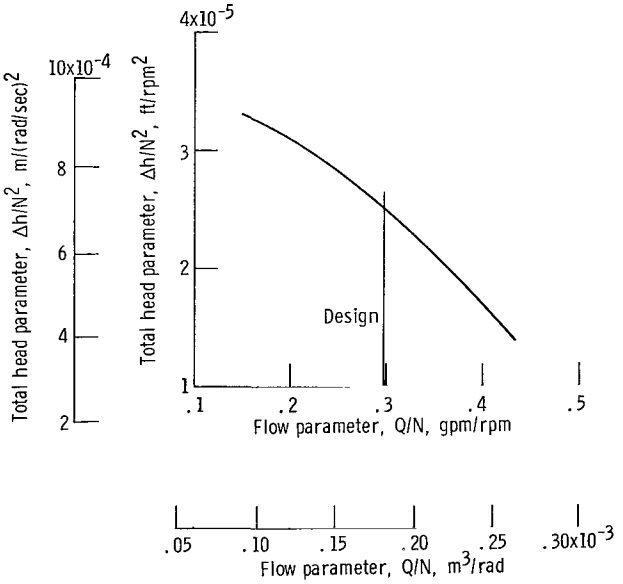

(a) Experimental generalized characteristic.

Figure 14. - Experimental generalized and analytically established pressurized startup characteristics for 3/8 scale model M-1 pump. Test fluid, water.

This characteristic, shown as the solid line in figure 14(b), has been extrapolated beyond its experimental range, down to $N/\dot{w} = 0$, as shown by the dashed line.

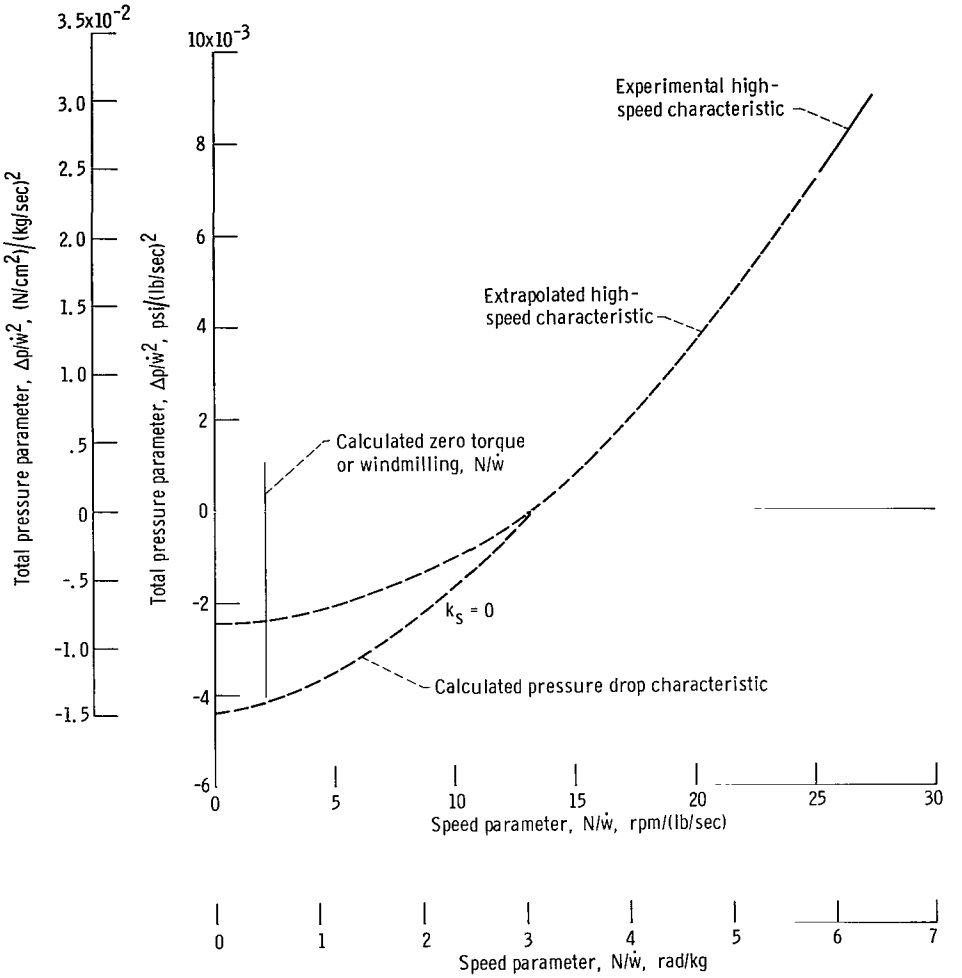

(b) Analytically established characteristic of pressurized startup.

Figure 14. - Concluded.

Pump design data and geometry, from unpublished data of Aerojet-General Corporation, are as follows:

Inlet tip diameter, in. (cm)	7.20 (18.3)
Inlet hub diameter, in. (cm)	3.24 (8.23)
Impeller discharge tip diameter, in. (cm)	10.69 (27.15)
Diffuser discharge diameter, in. (cm)	18.72 (47.5)
Impeller tip port, in. (cm)	0.855 (2.17)
Diffuser port, in. (cm)	0.908 (2.31)
Impeller vane blade discharge angle, deg	35
Discharge pipe diameter, in. (cm)	4 (10.16)
Nominal speed, rpm (rad/sec)	7480 (783)
Nominal flow, gpm (m^3/sec)	2141 (8.10)

Pressure drop characteristic. - The data listed in the previous section are used to calculate the loss coefficients and the ratio $y = V_2'/V_1$ for no slip operation at the design point. The negative head characteristics are calculated using equation (4a) with $k_s = 0$. The effect of the back vanes on the pump characteristic are neglected. After several intermediate steps of algebra, the pressure drop characteristic is

$$10^3 \frac{\Delta p}{\dot{w}^2} = -4.38 + 0.08 \left(\frac{N}{\dot{w}}\right) + \frac{1.89}{10^2} \left(\frac{N}{\dot{w}}\right)^2$$

$$10^2 \frac{\Delta p}{\dot{w}^2} = -1.47 + 0.116 \left(\frac{N}{\dot{w}}\right) + \frac{11.9}{10^2} \left(\frac{N}{\dot{w}}\right)^2$$

The calculated pressure drop characteristic of this pump is shown in figure 14(b) as the dashed line marked $k_s = 0$. Also indicated in this figure is the zero-torque point calculated using equation (5a).

Comparison of experimental and calculated data. - Examination of figure 14(b) indicates that the calculated pressure drop characteristic of the vaneless diffuser pump lies considerably lower than the extrapolated pump characteristic. As required, they meet at the line $\Delta p = 0$. No correction of the calculated performance line is required or possible because there are no vanes in the diffuser and the coefficient $k_s = 0$. This qualitative evaluation of the startup performance of a vaneless diffuser pump verifies the validity of the assumptions on which the diffuser entrance loss coefficient was calculated.

CONCLUDING REMARKS

An analytical method for calculation of startup characteristics of centrifugal pumps is presented. The hydrodynamic calculation of the pressure drop characteristic (when the pump is acting as a hydraulic turbine) is refined by use of an empirical constant to account for losses not predictable by analysis. The correction factor is obtained by modifying one parameter in the analytical equations until the calculated curve meets or closely approaches the extrapolated experimental pump characteristic at the point where the change in total pressure $\Delta p = 0$.

The method is verified by test runs on two types of pumps using liquid hydrogen. In both cases, the calculated pressure drop characteristics and the calculated zero-speed point, when corrected for diffuser entrance losses by the empirical constant, correlate satisfactorily with the experimental data.

The method has been applied also to a vaneless diffuser pump to illustrate the influence of the design parameters on the ability to predict the negative head characteristic. Because windmilling test data of the vaneless diffuser pump were not available, this evaluation is purely qualitative.

Lewis Research Center,
National Aeronautics and Space Administration,
Cleveland, Ohio, October 3, 1968,
731-11-03-03-22.

APPENDIX A

SYMBOLS

(Symbol lb is used for both pound force and pound mass.)

b	blade height, ft (m)
c	meridional blade length, ft (m)
D	diameter, ft (m)
d_h	hydraulic diameter, $2sb/(s + b)$, ft (m)
f	Fanning friction coefficient
g	acceleration due to gravity, ft/sec^2 (m/sec^2)
g_c	dimensional conversion factor, 32.17 (lbm)(ft)/(lbf)(sec^2)
Δh	change in total head, ft (m)
i	fluid incidence angle, $\beta_3 - \alpha_3$, deg
K	diffuser loss coefficient, $\frac{2g\,\Delta h_{loss}}{V_3^2}$
K_s	λk_s
$k_{f,r}$	impeller frictional loss coefficient
$k_{f,s}$	diffuser frictional loss coefficient
k_r	impeller inlet loss coefficient
k_s	diffuser inlet loss coefficient
N	rotational speed, rpm (rad/sec)
Δp	change in total pressure, psi (N/cm^2)
Q	volumetric flow rate, ft^3/sec or gpm (m^3/sec)
r	mean blade radius from axis of rotation, ft (m)
s	blade spacing, ft (m)
u	tangential velocity at mean blade diameter, $Nr/30$, ft/sec (m/sec)
V	absolute fluid velocity, ft/sec (m/sec)
V'	relative fluid velocity, ft/sec (m/sec)
W	work, ft-lb (J)
$\dot{w}$	flow rate, lb/sec (kg/sec)
y	proportionality constant, V_2'/V_1
Z_r	number of impeller vanes
Z_s	number of diffuser vanes
α	absolute fluid flow angle with respect to tangential direction, deg
α'	relative fluid flow angle with respect to tangential direction, deg
β	blade angle, deg
η	efficiency
λ	empirical correction factor for stator inlet loss
φ	viscous loss term, ft-lb/lb (m-N/kg)
Ω	flow area, ft^2 (m^2)

Subscripts:

a	axial component

d	design
e	pump exit
i	pump inlet
loss	refers to loss
s	static
u	tangential component
1	rotor inlet
2	rotor outlet
3	diffuser inlet
4	diffuser outlet

APPENDIX B

PERFORMANCE OF AN AXIAL FLOW, LIQUID HYDROGEN PUMP DURING STARTUP

NASA TM X-1213 (ref. 2) covers an analytical prediction and test verification of the performance of an axial flow liquid hydrogen pump during startup. Because of close similarity of startup analysis of the axial flow pump and the centrifugal pumps, the data contained in this appendix will help to understand the approach used in studies of centrifugal pumps.

The axial flow pump analyzed was the Mark IX liquid hydrogen pump. The pump is composed of an axial entrance, mixed flow, axial discharge inducer stage, and six identical high-pressure axial flow stages (except that the last rotor discharges directly into a vaneless volute). The equation for the generalized negative head characteristic is quite similar to equation (3). In calculations, the stator loss coefficient k_s was not corrected, that is, the stator entrance losses were assumed to be negligible at the design point.

Equation (5a) was used to calculate the zero-torque or windmilling point. Calculations were performed using assumptions of the design point deviation and assumptions of no deviation on pump blading.

Tests were performed in a liquid hydrogen facility equipped with a large overhead run tank, a turbopump stand, and a hydrogen disposal system. Tests included three pressure levels in the run tank. The windmilling tests were followed by bootstrap tests. A number of data points were obtained with pump being driven by a gas turbine in both the power dissipation zone and the pump operation zone.

Test Results

Figure 15 gives the zero-speed (locked rotor) and zero-torque (steady windmilling) calculated performance and corresponding test data. The zero-speed data verify the analytically established zero-speed curve (using the design point deviation assumption). The zero-torque or windmilling data fell short of the predicted characteristic.

Figure 16 shows the startup performance data in liquid hydrogen as well as the calculated characteristic (the dash-dotted line). The calculation was based on the assumption of design point deviation. The characteristic extending into the pump operation zone is the Mark IX pump characteristic. The solid line is experimental, while the dashed line is calculated (extrapolated) using a quadratic curve-fit equation of the experimental part of the characteristic. The rotation under windmilling conditions actually stabilized

at $N/\dot{w} = 192$ (44.3), while the calculated zero-torque point was $N/\dot{w} = 210$ (48.5). The difference should be attributed to mechanical loss torque not considered in the analysis. The zero-speed point is well verified. General agreement between the theory and experiment is good. It will be noticed that, in figure 16, the calculated pressure drop characteristic has a slope different from the pump characteristic and the two nearly meet at the line $\Delta p = 0$.

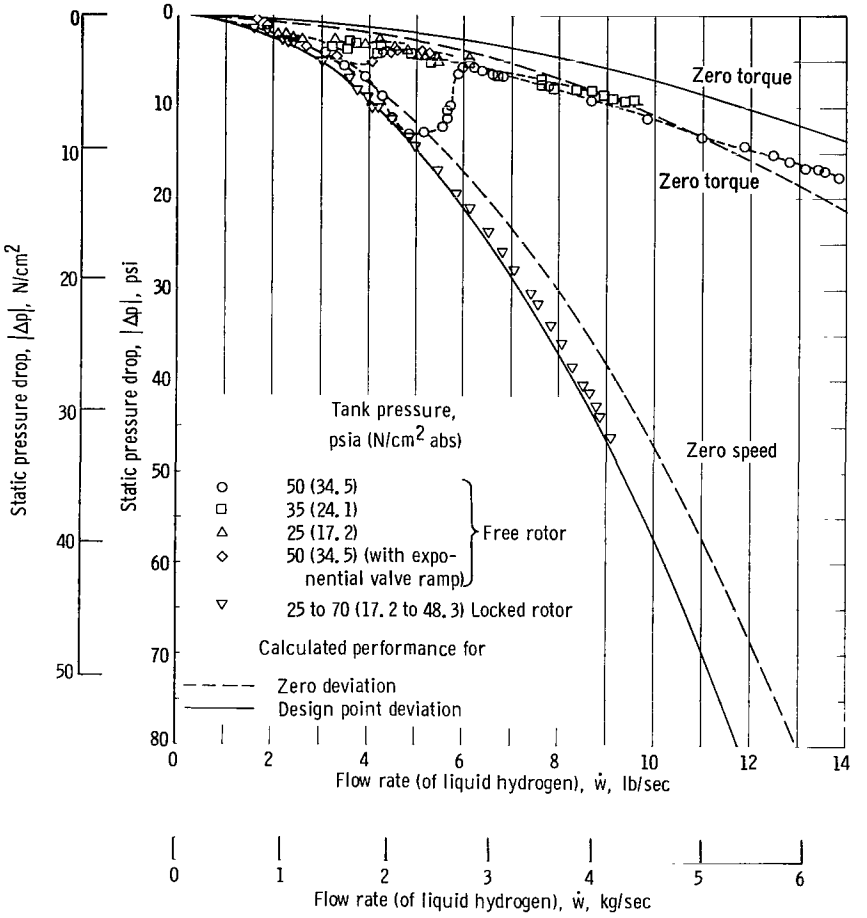

Figure 15. - Zero-speed (locked rotor) and zero-torque (steady windmilling) theoretical lines and corresponding test data.

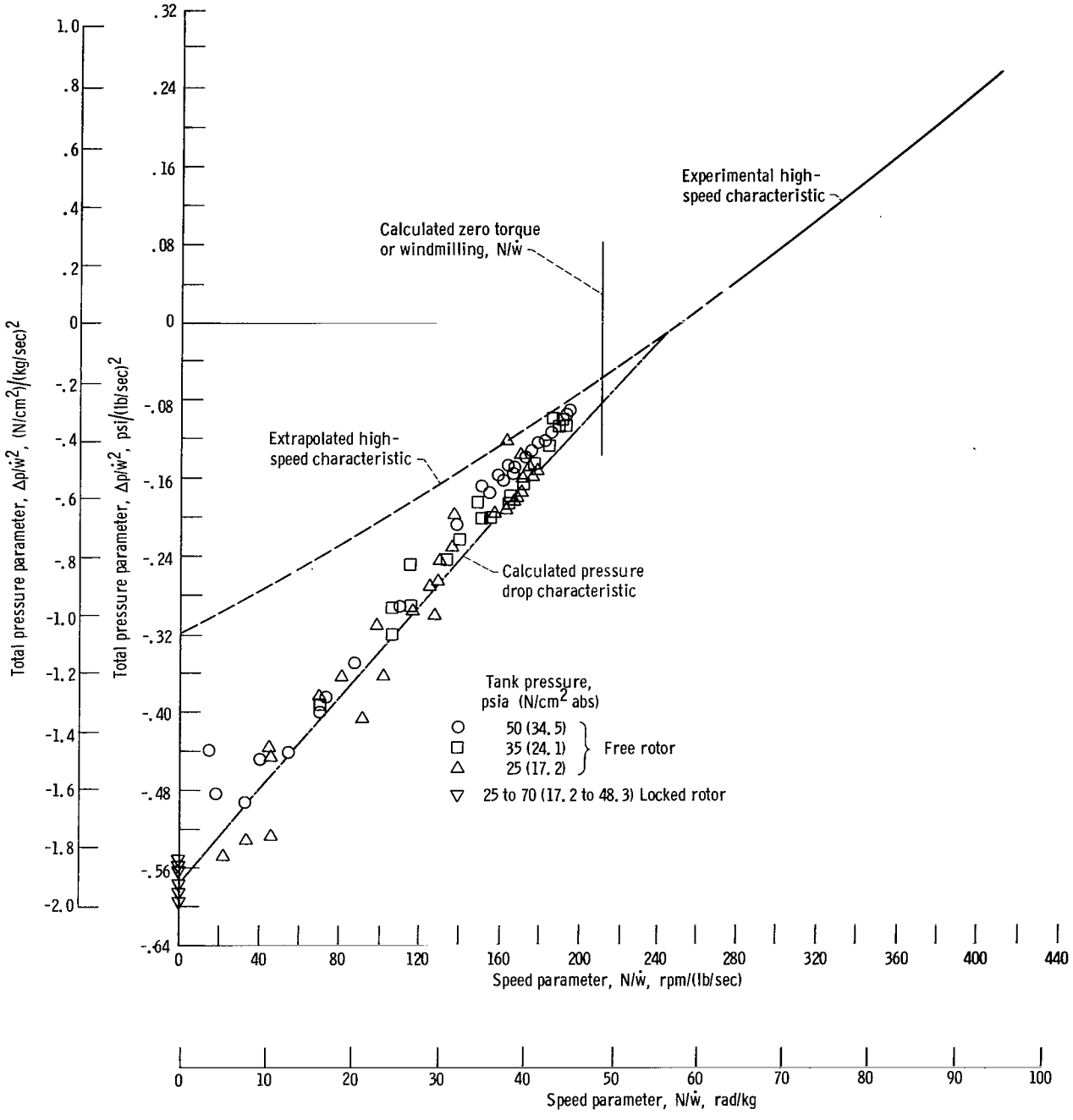

Figure 16. - Verification of analytically established characteristic for pressurized startup of Mark IX axial pump. Test fluid, liquid hydrogen.

APPENDIX C

LOSSES ASSOCIATED WITH VANED DIFFUSERS IN CENTRIFUGAL PUMPS

Unpublished data supplied by the Aerojet-General Corporation are given in figures 17 and 18 to illustrate the problem of evaluating losses associated with vaned diffusers in centrifugal pumps.

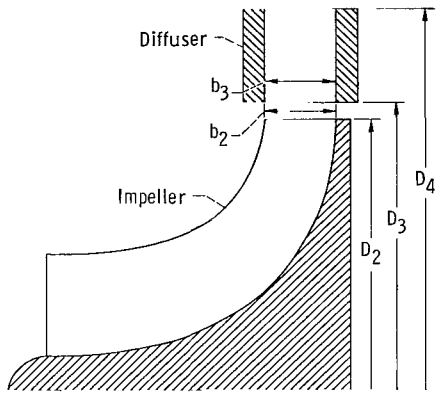

Test number	D_2, in.	D_2, cm	D_3, in.	D_3, cm	D_4, in.	D_4, cm	b_2, in.	b_2, cm	b_3, in.	b_3, cm	β_2, deg	β_3, deg	Number of impeller vanes, Z_r	Number of diffuser vanes, Z_s
-017	7.315	18.58	7.75	19.68	10.00	25.4	0.210	0.533	0.239	0.607	90	10	24	9
-014B	↓	↓	7.75	19.68	↓	↓	.315	.800	.375	.952	↓	↓	↓	↓
-015B	↓	↓	7.75	19.68	↓	↓	.315	.800	.375	.952	↓	↓	↓	↓
-022	↓	↓	7.95	20.19	↓	↓	.315	.800	.248	.630	↓	↓	↓	↓
-023	↓	↓	7.95	20.19	↓	↓	.210	.533	.248	.630	↓	6	↓	7

Figure 17. - Vaned diffuser configuration.

The Aerojet-General Corporation ran a series of tests on vaned diffusers to obtain data for off-design prediction of operation of the Mark III - Model IV turbopump. The diffuser vanes had essentially log-spiral mean camber lines from the leading edge to the vane overlap (throat) station and straight camber lines from this station to the trailing edge.

Loss coefficients were computed from measured average, upstream and downstream, static pressures and calculated velocities. The whirl velocity of the impeller fluid exit was assumed to be 90 percent of the wheel velocity, and the flow was assumed to follow the vane at the diffuser discharge.

Figure 17 shows the vaned diffusers used to analyze experimentally the off-design losses. This figure contains the geometry of the tested rotor-diffuser assemblies.

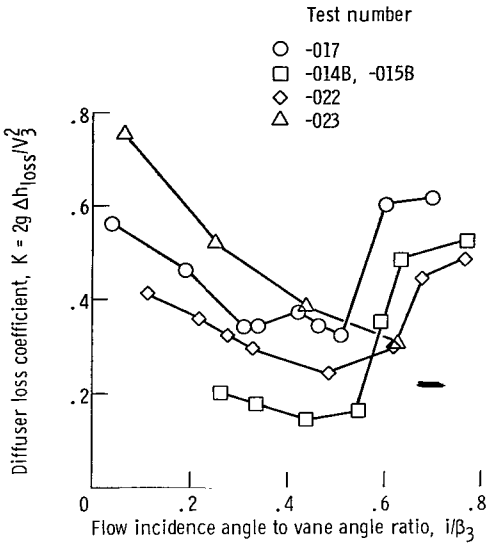

Figure 18. - Test results for vaned diffuser loss coefficient.

Figure 18 gives the experimental results. The tests have been run for positive incidence only. The minimum loss point cannot be correlated with any particular value of the ratio i/β_3. The minimum loss coefficient varies from 0.15 to 0.32, and this variation cannot be correlated with the geometrical data of the tested diffusers. To the right of the minimum loss point, the losses steeply increase; while to the left, the increase is gradual. From these data, it appears that the off-design performance of these pumps cannot be predicted.

REFERENCES

1. Rostafinski, Wojciech A.; and Rudey, Richard A.: Analytical Evaluation of Off-Design Performance of a Multi-Stage Axial-Flow Liquid-Hydrogen Pump. NASA TM X-1254, 1966.

2. Rostafinski, Wojciech; Rudey, Richard A.; Lacy, Donald D.; and Lillis, Patrick R.: Performance Characteristics of an Axial-Flow Liquid-Hydrogen Pump During Start-up. NASA TM X-1213, 1966.

3. Swanson, W. M.: Complete Characteristic Circle Diagrams for Turbomachinery. Trans. ASME, vol. 75, no. 5, July 1953, pp. 819-826.

4. Knudsen, James G.; and Katz, Donald L.: Fluid Dynamics and Heat Transfer. McGraw-Hill Book Co., Inc., 1958.

5. Daugherty, Robert L.: Hydraulic Turbines. Third Ed., McGraw-Hill Book Co., Inc., 1920.

NASA-Langley, 1968 —— 15 E-4254

"The aeronautical and space activities of the United States shall be conducted so as to contribute . . . to the expansion of human knowledge of phenomena in the atmosphere and space. The Administration shall provide for the widest practicable and appropriate dissemination of information concerning its activities and the results thereof."

— NATIONAL AERONAUTICS AND SPACE ACT OF 1958

NASA SCIENTIFIC AND TECHNICAL PUBLICATIONS

TECHNICAL REPORTS: Scientific and technical information considered important, complete, and a lasting contribution to existing knowledge.

TECHNICAL NOTES: Information less broad in scope but nevertheless of importance as a contribution to existing knowledge.

TECHNICAL MEMORANDUMS: Information receiving limited distribution because of preliminary data, security classification, or other reasons.

CONTRACTOR REPORTS: Scientific and technical information generated under a NASA contract or grant and considered an important contribution to existing knowledge.

TECHNICAL TRANSLATIONS: Information published in a foreign language considered to merit NASA distribution in English.

SPECIAL PUBLICATIONS: Information derived from or of value to NASA activities. Publications include conference proceedings, monographs, data compilations, handbooks, sourcebooks, and special bibliographies.

TECHNOLOGY UTILIZATION PUBLICATIONS: Information on technology used by NASA that may be of particular interest in commercial and other non-aerospace applications. Publications include Tech Briefs, Technology Utilization Reports and Notes, and Technology Surveys.

Details on the availability of these publications may be obtained from:

SCIENTIFIC AND TECHNICAL INFORMATION DIVISION

NATIONAL AERONAUTICS AND SPACE ADMINISTRATION

Washington, D.C. 20546